

**A peer-reviewed version of this preprint was published in PeerJ on 26 March 2019.**

[View the peer-reviewed version](https://peerj.com/articles/6657) (peerj.com/articles/6657), which is the preferred citable publication unless you specifically need to cite this preprint.

García-Jiménez B, Wilkinson MD. 2019. Robust and automatic definition of microbiome states. PeerJ 7:e6657 <https://doi.org/10.7717/peerj.6657>

# Automatic definition of robust microbiome sub-states in longitudinal data

Beatriz García-Jiménez <sup>Corresp., 1, 2</sup>, Mark D Wilkinson <sup>1</sup>

<sup>1</sup> Biological Informatics Group, Centro de Biotecnología y Genómica de Plantas UPM-INIA, Universidad Politécnica de Madrid, Madrid, Spain

<sup>2</sup> Systems Biotechnology Group, Centro Nacional de Biotecnología, Spanish National Research Council, Madrid, Spain

Corresponding Author: Beatriz García-Jiménez  
Email address: [beatriz.garcia@csic.es](mailto:beatriz.garcia@csic.es)

The analysis of microbiome dynamics would allow us to elucidate patterns within microbial community evolution; however, microbiome state-transition dynamics have been scarcely studied. This is in part because a necessary first-step in such analyses has not been well-defined: how to deterministically describe a microbiome's "state". Clustering in states have been widely studied, although no standard has been concluded yet. We propose a generic, domain-independent and automatic procedure to determine a reliable set of microbiome sub-states within a specific dataset, and with respect to the conditions of the study. The robustness of sub-state identification is established by the combination of diverse techniques for stable cluster verification. We reuse four distinct longitudinal microbiome datasets to demonstrate the broad applicability of our method, analysing results with different taxa subset allowing to adjust it depending on the application goal, and showing that the methodology provides a set of robust sub-states to examine in downstream studies about dynamics in microbiome.

# Automatic Definition of Robust Microbiome Sub-states in Longitudinal Data

Beatriz García-Jiménez<sup>1,2</sup> and Mark D. Wilkinson<sup>1</sup>

<sup>1</sup>Biological Informatics Group, Centro de Biotecnología y Genómica de Plantas UPM-INIA, Universidad Politécnica de Madrid, Campus Montegancedo, 28223-Pozuelo de Alarcón (Madrid), Spain.

<sup>2</sup>Current affiliation: Systems Biotechnology Group, Centro Nacional de Biotecnología, Spanish National Research Council, C/ Darwin nº 3, Campus de Cantoblanco, 28049-Madrid, Spain.

Corresponding author:  
Beatriz García-Jiménez<sup>1,2</sup>

Email address: [beatriz.garcia@csic.es](mailto:beatriz.garcia@csic.es)

## ABSTRACT

The analysis of microbiome dynamics would allow us to elucidate patterns within microbial community evolution; however, microbiome state-transition dynamics have been scarcely studied. This is in part because a necessary first-step in such analyses has not been well-defined: how to deterministically describe a microbiome's "state". Clustering in states have been widely studied, although no standard has been concluded yet. We propose a generic, domain-independent and automatic procedure to determine a reliable set of microbiome sub-states within a specific dataset, and with respect to the conditions of the study. The robustness of sub-state identification is established by the combination of diverse techniques for stable cluster verification. We reuse four distinct longitudinal microbiome datasets to demonstrate the broad applicability of our method, analysing results with different taxa subset allowing to adjust it depending on the application goal, and showing that the methodology provides a set of robust sub-states to examine in downstream studies about dynamics in microbiome.

## INTRODUCTION

This manuscript addresses an important challenge in microbiome analysis: identification and description of longitudinal microbiome variability and dynamics (Gilbert et al., 2016; Bashan et al., 2016; Bradley and Pollard, 2017). Microbiomes are distinct between different cavities (or more generally, distinct environments) (Bashan et al., 2016). One widely-accepted view of the microbiome within a given cavity is to consider it from a global perspective - that among all individuals there is one shared state, broadly-defined, but internally-variable and dynamic (Gibbons et al., 2017). With respect to the gut microbes, there were initial attempts to resolve distinct microbial population structures that were associated with "habits" such as lifestyle, culture, or eating - called "enterotypes". Albeit, there is a big discussion about enterotypes (whether, how many and which ones) (Costea et al., 2018). Some studies are agree with discrete states (Zhou et al., 2014; Turrone et al., 2017), while other ones with gradients (MacDonald et al., 2012; Gibbons et al., 2017). It is well-recognized that distinct and predictable microbial compositions are associated with important traits such as health (Gilbert et al., 2016; Shankar, 2017). Nevertheless, even if there were no universally-distinct enterotypes, this would not imply that microbiomes cannot exist in long- or short-term stable sub-states. Moreover, within a given individual, studies suggest the existence of such stable steady-states, both in experimental data (Turrone et al., 2017) and in modeling approaches (Stein et al., 2013; Bashan et al., 2016), not considering a state as a constant community composition but an average along a period of time (Chan et al., 2017). As such, the proposition of a single, but continuously varying, microbiome state within a given environment fails to recognize subtle differences that may have significant biological consequences. Thus, the definition of several sub-states could help to capture slight microbiome shifts, happened even in a general stability situation, and undetectable in other approximations, where only one state or a few with strong divergence were considered.

47 Faust et al. (2015) reported that microbial diversity was quite stable over time, in a stable environment,  
48 but that stability could be disrupted by a) external perturbations, b) direct modifications or c) transient  
49 perturbations, all of which cause the microbial community to change. Longitudinal studies focused on  
50 microbiome changes over time, in a particular habitat, with known interventions, would elucidate the  
51 mechanisms behind microbial state transitions, and from this information, universal or context-specific  
52 interventions could be determined (Bashan et al., 2016), and used to manipulate the microbiome in  
53 desirable ways. Thus a domain-independent (e.g. human/animal body cavities, soils, industrial microbial  
54 communities in bioreactors, etc.) and flexible approach to analysis of longitudinal microbiome variability  
55 and dynamics is needed.

56 In this manuscript, we define a microbiome "sub-state" as a collection of constraints satisfied by  
57 the microbiota of a given sample, that are not satisfied by other samples, allowing them to be reliably  
58 distinguished from one another. Thus, over time, and depending on perturbations, a dynamic microbial  
59 community could move through different microbiome sub-states, even within a single "enterotype" as  
60 defined by Arumugam et al. (2011b) (or its conceptual equivalent in non-gut environments). Thus, we  
61 consider microbiome sub-states to be akin to biomarkers, and importantly, these biomarkers differ between  
62 individuals or even within the same one, as "a measurable indicator of a biological state or environmental  
63 exposure" (Gorvitovskaia et al., 2016). Finally, our definition of microbiome sub-state describes the  
64 microbial community composition over a specific fragment of time.

65 There are relatively few studies about temporal dynamics within any microbiome site (Gajer et al.,  
66 2012; Ding and Schloss, 2014), and for those studies, the approach to microbiome sample clustering is  
67 assorted and somewhat *ad-hoc*. This masks the fact that the definition of states in a temporal sequence  
68 of microbiomes is non-trivial, and has only been attempted within specific datasets (Koren et al., 2013).  
69 Therefore, we believe that a generally-applicable algorithm that detects robust and stable microbiome  
70 sub-states within any input dataset, would be a beneficial contribution to the community, and would aid in  
71 the cross-replication and comparison of studies in the future. We report such a methodology here.

72 The inputs to our pipeline are Operational Taxonomic Unit (OTU) vectors, where each OTU represents  
73 a group of species considered indistinguishable by the OTU grouping process, and whose abundance  
74 in a set of samples has then been computed. Given that these abundance distributions are effectively  
75 continuous, the list of possible OTU combinations as possible sub-states clearly must be simplified to  
76 ensure that the space of the OTU vector is so large as to be computationally intractable. On the other hand,  
77 increasing simplification results in an vanishingly small numbers of sub-states, which are insufficiently  
78 granular as to occur in any "biologically meaningful" association. This is, therefore, the key consideration  
79 when defining the approximation for grouping similar OTU vectors, for example, by machine learning  
80 clustering approaches. Effectively, our choice of clustering parameters should be guided by the desire  
81 to identify several well-populated microbiome sub-states both within and between individuals, which  
82 can then be used as the basis of a model associating these sub-states with various biologically interesting  
83 phenomenon. It should be noted that this is a distinct goal from that of most microbiome studies, which  
84 consider the stable-state microbiome as a single entity (e.g. the enterotype studies). As such, the 'default'  
85 clustering parameters that appear in most published approaches do not match our problem requirements,  
86 and must be re-considered from scratch.

87 Our overall procedure for defining sub-states, described in detail below, consists of applying a  
88 clustering algorithm to the OTU data, taking a metagenomics beta diversity metric as the distance measure  
89 between samples. We then attempt to robustly define the optimal number of clusters based on a comparison  
90 between several distance measures, distinct algorithms and different clustering scores.

91 Metagenomics sample clustering has been achieved for different studies using a variety of approaches,  
92 in terms of distance measure, algorithm and number of clusters. For example, as a distance measure, the  
93 Jensen-Shanon Distance (JSD) (or its root squared, rJSD, as in (Arumugam et al., 2011b)) is the most  
94 frequently used (Gajer et al., 2012); although the cophenetic or the Euclidean distance are also sometimes  
95 applied. Several clustering algorithms have been used to group metagenomics samples, such as PAM,  
96 Agnes, Hclust, or Dirichlet Multinomial Mixture, with different linkage options (Ding and Schloss, 2014).  
97 For determination of the number of clusters, diverse assessment criteria have been used in the literature:  
98 the average Silhouette width (SI), Calinski-Harabasz (CH) index, Laplace approximation, etc. In the  
99 specific case of enterotypes, clustering of samples was applied (Arumugam et al., 2011b). According their  
100 tutorial (Arumugam et al., 2011a), they computed the distance as the root square of the JSD, with the  
101 PAM algorithm and selecting the number of clusters with the CH index combined with a SI assessment.

102 Conversely, Gajer et al. (2012) applied hierarchical clustering with JSD and SI assessment.

103 This manuscript describes an algorithm consisting of several consecutive steps, where the most robust  
104 set of sub-states (or clusters) is generated for a given longitudinal microbiome dataset. Briefly, the  
105 variable factors that are combined to generate the robustness of our algorithm include: five different  
106 distance measures (JSD, rJSD, Bray-Curtis, Morisita-Horn and Kulczynski), two clustering scored (SI  
107 and Prediction Strength (PS) scores) followed by an additional bootstrapping process (evaluated with the  
108 Jaccard similarity score), and two distinct clustering approaches (PAM and Hclust).

109 The usability of the proposed new algorithm is verified through the re-analysis of four previously-  
110 published longitudinal microbiome datasets, where we contribute new insights into the dataset structure,  
111 and show that sub-state distribution could be further reused by other kinds of downstream associative  
112 analyses of the same datasets.

113 The contribution of this work, therefore, is to provide an objective and robust mechanism for identify-  
114 ing, and tracking, distinct sub-states and sub-state changes within an individual microbiome time series.  
115 This will enable downstream analyses about what, how and why transitions between sub-states happen,  
116 and this could in-turn address the challenge of applying microbiota dynamics to important objectives such  
117 as personalized medicine (Gilbert et al., 2016), sustainable agriculture or industrial production (Valseth  
118 et al., 2017).

## 119 MATERIALS AND METHODS

### 120 Algorithm: Automation of the robust sub-states definition

121 This section describes a brief overview of our automatic procedure to define microbiome sub-states. Our  
122 robust clustering methodology takes a normalized OTU matrix as input: a) a phyloseq object (McMurdie  
123 and Holmes, 2013) or b) a BIOM format file (McDonald et al., 2012), together with their corresponding  
124 metadata that identifies each sample and taxa.

125 Our clustering procedure is based on: 1) Koren et al. (2013)'s study 2) bootstrapping in clustering,  
126 and 3) similarity measures from (Barwell et al., 2015). Koren et al. (2013) recommends, for the definition  
127 of enterotypes, testing multiple approaches and comparing results. Following these suggestions, our  
128 algorithm first finds clusters using two different methods (PAM and Hclust), with five different distance  
129 metrics (JSD, root-JSD, Bray-Curtis, Morisita-Horn and Kulczynski) each, and with nine different seed  
130 cluster numbers,  $k$  (in the range from 2 to 10).

131 From the output of this first step, we begin to identify the most robust results through a novel  
132 assessment approach that utilizes the following criteria:

- 133 1. Choosing the  $k$  number of clusters (from 2 to 10) with the highest average Silhouette width (SI)  
134 among all combinations of pairs of beta diversity measures, with the score being above the SI  
135 threshold (0.25), and
- 136 2. Checking if that  $k$  value also passes the Prediction Strength (PS) threshold (0.80) for robustness, or
- 137 3. Confirming if those  $k$  clusters are stable according to the Jaccard threshold (0.75) from a bootstrap-  
138 ping process

139 Those criteria are applied to the output of the 90 combinations (2 algorithms x 5 distances x 9  $k$  values)  
140 per dataset, in order to discard those that are not robust and/or not reproducible. Next sections explains  
141 the steps in detail, and the relevant factors within our automatic procedure. In particular, we adapt the  
142 Koren et al. (2013) approach to the distinct problem of defining microbiome states that exhibit short-term  
143 transitions within the same individual, rather than the long-term stereotypes common to enterotype studies,  
144 with sparse transitions and where each individual has just one associated state.

145 The final output of our algorithm is a phyloseq object with a new variable defining the cluster identifier  
146 into which each sample has been grouped, a file with <sampleID, clusterID> pairs, and the robust  
147 clustering assessment graphs (described below).

### 148 Clustering approaches

149 We selected these two algorithms as representatives of the two most common clustering approaches:  
150 a) PAM (Kaufman and Rousseeuw, 1990), as a partitioning approach, and b) Hclust (Kaufman and  
151 Rousseeuw, 1990), as an agglomerative hierarchical approach.

152 We selected PAM (Partitioning Around Medoids) (Kaufman and Rousseeuw, 1990) because it is an  
153 improved approach to the well-known non-deterministic  $k$ -medoids (Kaufman and Rousseeuw, 1987).  
154 This improvement is achieved in two ways. First, PAM selects  $k$  medoids among the input instances in a  
155 greedy phase, rather than the random selection of the  $k$ -medoids approach (Reynolds et al., 2006). The  
156 greedy phase takes each new medoid to minimize the objective function, that is, the sum of distances  
157 between each instance and its medoid. Therefore, PAM is a deterministic algorithm and does not need  
158 to be run multiple times, as is the case for  $k$ -medoids. Second, it spreads out the rest of the instances  
159 among the defined medoids according to the minimum distance-to-medoid criterion, using the values  
160 defined in the distance matrix. PAM then selects each possible pair of instances  $\langle \text{medoid}, \text{not-medoid} \rangle$ ,  
161 and evaluates whether the swapping between different clusters results in a smaller value for the objective  
162 function. This final step is repeated until the set of medoids do not change.

163 Hclust, a hierarchical clustering algorithm, adopts a *bottom-up* approach (Kaufman and Rousseeuw,  
164 1990). Hclust begins with an independent cluster per instance. The two nearest clusters are then grouped,  
165 in an iterative way, until it arrives at a single cluster, which is therefore the root of an inverted tree  
166 structure. We chose *average* (i.e. UPGMA) distance between cluster members as the linkage criteria used  
167 to compute the distance between two clusters, rather than single or complete linkage which takes only  
168 one cluster element into account when computing the distance (Kaufman and Rousseeuw, 1990).

### 169 **Beta diversity metrics or distance measures**

170 We took Koren et al. (2013)'s study as reference, because they evaluated beta diversity metrics' influence  
171 on the clustering results of microbiome samples, which is similar to our goal here. They recommended  
172 comparing at least 2 or 3 different distance measures in the clustering process; we chose to compare 5  
173 distinct measures. Those were chosen from a large list available in the R vegan package (version 2.3-1)  
174 (Oksanen et al., 2015), based on suggestions from the work of Koren et al. (2013) and a comprehensive  
175 study ranking all available beta diversity measures with abundance data (Barwell et al., 2015), which  
176 compared multiple quantitative and qualitative properties.

177 First, we selected well-extended Jensen-Shanon Distance (**JSD**), **rootJSD** and **Bray-Curtis**, due  
178 to they are used in our reference study (Koren et al., 2013). Then, in addition, because our method is  
179 independent of the availability of a phylogenetic tree associated to the OTU count matrix, we choose 2  
180 additional metrics from Barwell et al. (2015) to replace the phylogenetic tree-dependent Unifrac metric  
181 (weighted and unweighted) used by (Koren et al., 2013). Although there was a precedent study with  
182 23 presence-absence beta diversity metrics (Koleff et al., 2003), we decided to focus on the richer  
183 metrics with continuous species abundance Barwell et al. (2015). In general, abundance metrics are  
184 less biased than presence-absence ones when under-sampling. (Barwell et al., 2015) compares 29 beta  
185 diversity measures with 23 assorted properties. We chose the **Morisita-Horn** and **Kulczynski** metrics  
186 from amongst the almost thirty analyzed metrics, taking into account the overall ranking and some specific  
187 individual properties that are more important for our use of beta diversity metrics as distance measures in  
188 clustering. Morisita is the highest scored beta diversity measure according to the comprehensive set of  
189 properties analyzed in Barwell et al. (2015); although we must select the Morisita-Horn implementation  
190 (the third best scored) since we work with normalized relative abundances. In addition, both Morisita and  
191 Horn-Morisita have been described as being "able to handle different sample sizes" (Wolda, 1981), which  
192 is an important characteristic in our studies, where the re-used longitudinal microbiome datasets vary  
193 dramatically in size. Kulczynski, meanwhile, is the next-best ranked metric among those available in the  
194 R vegan package, ranking sixth out of 29 metrics. Kulczynski is characterized as Pareto-dominant, and  
195 "found to have a robust linear (proportional) relationship until ecological distances became large" (Faith  
196 et al., 1987).

### 197 **Clustering assessment scores**

198 Koren et al. (2013) recommend using at least two assessment clustering scores. The three different,  
199 complementary clustering scores we selected, and how they are included in our automatic procedure, are  
200 as follows:

- 201 1. **SI: average Silhouette width:** First, we search for the  $k$  number of clusters with the best SI, with  
202  $k$  limited to the range of 2 to 10. This first step was also taken in a previous study, computing  
203 microbiome states in a particular dataset (Gajer et al., 2012). Here, we compute the average of all  
204 possible combinations of SI values for two different distance measures and each  $k$ , selecting that

205 one with the highest average. The average SI must be greater than 0.25 in all selected measures,  
206 because it is the minimum threshold for ‘sensible’ clusters, according to (Rousseeuw, 1987). This  
207 score takes into account the similarity between the samples in the same and in the nearest clusters.  
208 If the selected pair of distance measures does not outperform the following robustness constraint,  
209 the next best combination is checked.

210 2. **PS: Prediction Strength:** Although Koren et al. (2013) indicate that clustering selection could be  
211 restricted just to SI score in small datasets, we include this alternative, PS, which is also used in  
212 Koren et al. (2013). Our method runs 100 repetitions where the dataset is split into 2 halves and  
213 clustering is applied on both; then we search for a correspondence between both group of clusters,  
214 classifying points in half A to cluster in half B and vice-versa. Each pair is considered as well  
215 classified if both points are classified to the same cluster in the other half. The score is the frequency  
216 of correct classification pairs.

217 3. **Jaccard similarity:** Though the computation of PS implies some kind of bootstrapping, our  
218 methodology allows an alternative, explicit bootstrapping step, to verify the stability of the clusters  
219 selected with the previous scores. This bootstrapping consists of a resampling with replacement,  
220 where clustering is computed over the whole dataset and, in addition, again 100 resamples. Since  
221 the Jaccard score compares groups of elements, we computed the similarity of the original cluster  
222 with each resampling cluster. Thus, the resulting similarity score is the mean of the size of the  
223 intersection divided by the size of the union of samples.

224 In summary, a total of 18,090 different clustering processes are executed to decide the best microbiome  
225 sub-states in a specific dataset. 18.090 comes from 9 ( $k = 2 : 10$ ) potential number of clusters x 5 distance  
226 measures (JSD, rJSD, Bray-Curtis, Morisita-Horn and Kulczynski) x 201 assessment scores (1 SI + 100  
227 PS + 100 Jaccard) x 2 clustering algorithms (PAM and Hclust).

228 Clustering and the distances between OTU vectors were computed with the implementation of different  
229 R packages, including the *distance* function in the *phyloseq* R package (v1.19.1) (McMurdie and Holmes,  
230 2013), the *pam* function in the *cluster* R package (v2.0.6), the *hclust* function in the *stats* R package  
231 (v3.4.3). Those algorithms take, as input, a distance matrix, where we use the metagenomics beta diversity  
232 measures comparing samples, rather than a  $\{samples \times features\}$  matrix as required by other algorithms.  
233 The first clustering assessment was computed with the *silhouette* function in the *cluster* R package; the  
234 robustness evaluation is computed with the *prediction.strength* function (Tibshirani and Walther, 2005)  
235 and the corresponding bootstrapping scored by Jaccard similarity with the *clusterboot* function (Hennig,  
236 2007, 2008), both in *fpc* R package (v2.1-11).

## 237 RESULTS

238 This section describes the application in identifying robust clusters in previously published longitudinal  
239 microbiome datasets. For each reused dataset, we first show its microbiome sub-state definition and  
240 evaluation, followed by a brief interpretation of the clusters (if feasible).

### 241 Human gut microbiome sub-states

242 The dataset from David et al. (2014) is, to our knowledge, the longest and most frequently sampled  
243 longitudinal study of the human gut microbiome in healthy subjects. Briefly, it consists of near-daily  
244 stool sampling of two distinct subjects, throughout an entire year, including 493 gut samples with 4746  
245 taxa. The input OTU table with absolute abundances was kindly shared by the authors in a personal  
246 communication. Dataset details and availability are provided in the Data Citation section.

247 This and the subsequent sub-sections show the three complementary clustering assessment steps  
248 defined in section *Algorithm: Automation of the robust sub-state definition* (corresponding to the three  
249 columns in Fig 1), with two different clustering approaches, and five distinct diversity metrics (corre-  
250 sponding to the colored lines).

251 Figure 1 contains the following analyses:

252 1. The first column shows the results of the algorithms attempt to choose the most suitable number  
253 of clusters,  $k$ , according to distinct beta diversity measures (i.e. distance among samples) scored  
254 according to SI. The selected  $k$  value (from 2 to 10) must report the highest average SI in the best

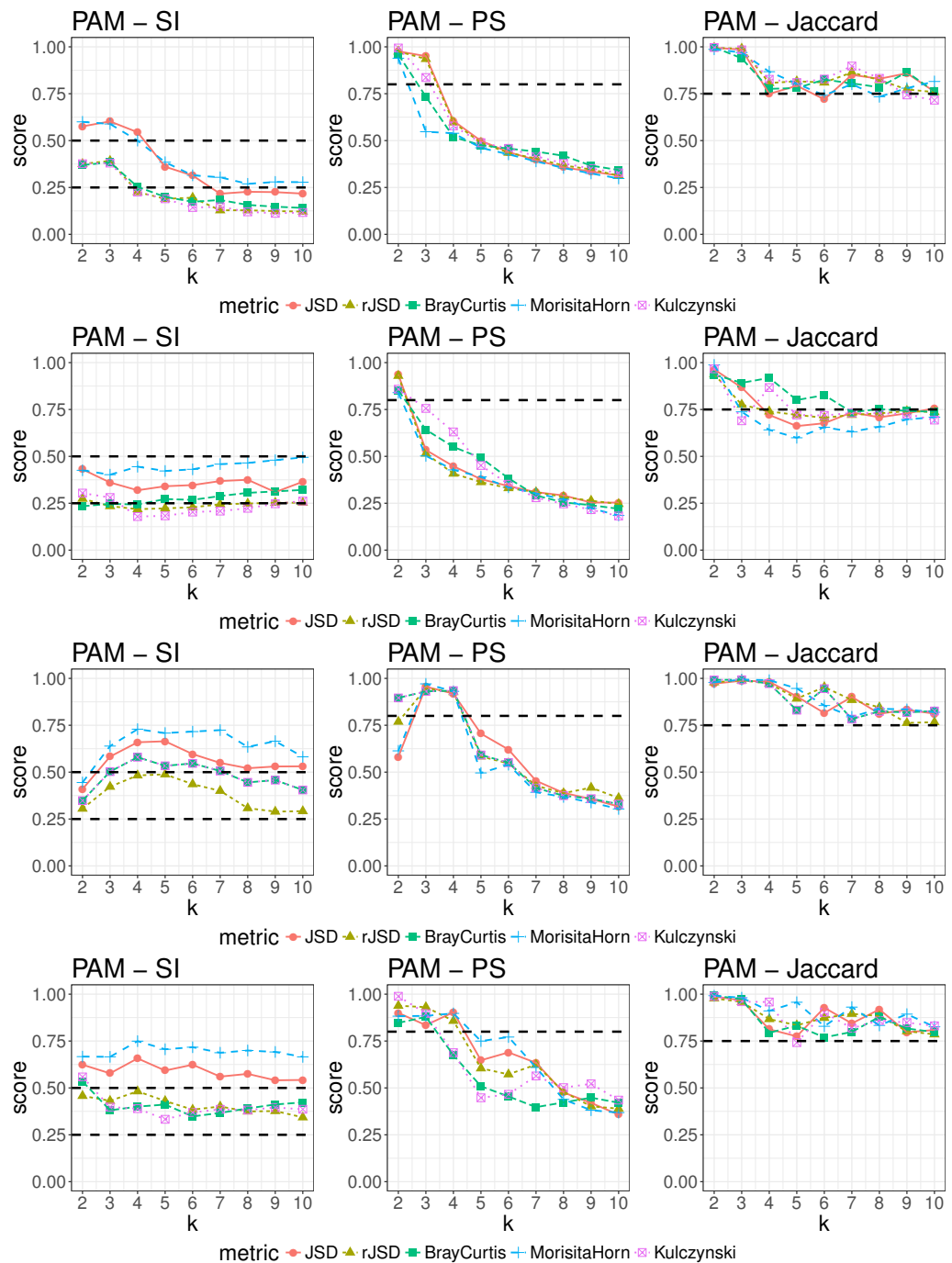


**Figure 1. Robust clustering evaluation, with PAM algorithm, in different datasets.** From top to bottom: (1) Human gut microbiome (David et al., 2014), (2) Chick gut (Ballou et al., 2016), (3) Vagina (Gajer et al., 2012), (4) Preterm infant gut (La Rosa et al., 2014).



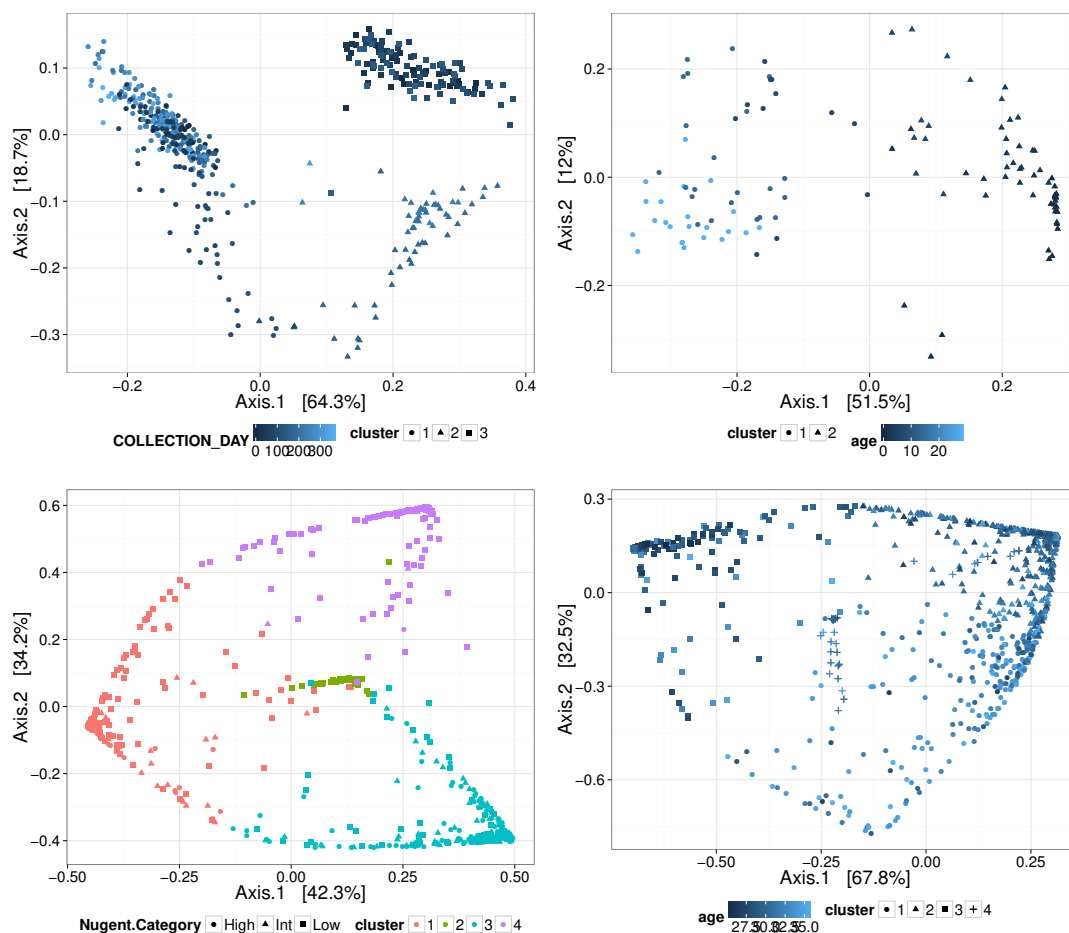


**Figure 2. Clusters represented as Principal Coordinates graphs.** A (up left): Human Gut. B (up right): Chick Gut. C (bottom left): Vagina. D (bottom right): Preterm Infant Gut.

255 pair of two beta diversity measures. In Fig 1.1, first column, the selected number of clusters is  
 256  $k=3$ . With 3 clusters, SI takes its highest value (0.602) when utilizing the PAM algorithm (top  
 257 row), and the JSD metric; the remainder metrics are also higher than the minimum threshold, with  
 258 Morisita-Horn being the second best metric, scoring above the threshold for strong clusters.

259 2. The second column allows us to check if the  $k$  value chosen by SI in the former step is sufficiently  
 260 robust, by testing it against the PS criterion of being greater than 0.8. The second column of  
 261 Fig 1.1 shows that JSD and rJSD in PAM with  $k=3$  satisfies the robustness test with  $PS=0.950$  and  
 262  $PS=0.935$ . At  $k=4$ , however, the PS value decreases to the point where the threshold is not passed  
 263 using any other metric, despite being acceptable based on the SI.

264 3. Finally, the third column reinforces the stability of the selected  $k$  clusters, by testing if the Jaccard  
 265 similarity of the chosen diversity measures exceed 0.75. The last column of Fig 1.1 verifies the  
 266 stability criterion, with Jaccard=0.986 for the selected  $k=3$  clusters for JSD and, in this case, also  
 267 for all remaining beta diversity metrics.

268 **Cluster interpretation:** Fig 2 shows, as Principal Coordinates (PCoA) graphs, the final set of clusters  
 269 selected by our algorithm for each dataset. Fig 2.A shows the 3 sub-states (clusters) that could be  
 270 associated to an annotated biological phenomenon. In this case, the associations are with:  $\{subject A,$   
 271  $subject B$  before dysbiosis,  $subject B$  after dysbiosis $\}$ . No further interpretation was possible using this  
 272 complicated dataset because insufficient additional metadata was available to test for association.

### 273 Chick gut microbiome sub-states

274 The second dataset was generated by Ballou et al. (2016). It analyses the response of the developing  
275 chick gut microbiome to different treatments (salmonella vaccine and/or probiotics) during their first  
276 month of life. The dataset consists of 119 samples with 1583 taxa. The samples include six time points,  
277 with 4 or 5 subjects per each of the four treatment combinations. Our goal, therefore, was to define the  
278 natural groupings of chick gut microflora. Dataset details and availability are provided in the Data Citation  
279 section.

280 **Clustering assessment:** Fig 1.2 shows that two clusters are identified by our method;  $k=2$  presents  
281 the highest SI value (0.431) in PAM with the JSD metric (with additional metrics above the 0.25 limit)  
282 (first column), and also passes the robustness threshold of PS with 0.935 (second column) and the stability  
283 threshold of Jaccard similarity with 0.964 (third column).

284 **Cluster interpretation:** Fig 2.B shows that the 2 clusters largely correspond to *immature/young*  
285 chicks and *mature/adult* chicks, reinforcing the conclusion of the original manuscript, which showed  
286 chick age to be the primary differential factor among samples.

### 287 Vaginal microbiome sub-states

288 The Gajer et al. (2012) dataset consists of 937 samples and 330 OTUs, corresponding to 32 women,  
289 with samples collected twice per week for 16 weeks. Dataset details and availability are provided in the  
290 Data Citation section. In this case, the original data counts are already pre-processed, and normalized  
291 to a sum of 100 per sample, as relative abundances. This contrasts with the previous datasets, where a  
292 normalization procedure was applied by us before entering the data into our algorithm.

293 **Clustering assessment:** In the Gajer et al. (2012) dataset, our methodology determines that the  
294 strongest sample groups appear with 4 clusters, with the highest SI value (0.730) resulting from the  
295 clustering with PAM and Morisita-Horn metric. They similarly fulfil the robustness and stability criterion,  
296 with PS=0.931 and Jaccard=0.990, respectively, as Fig 1.3 shows.

297 **Cluster interpretation:** Our method defines 4 clusters (see Fig 2.c) rather than the 5 clusters identified  
298 in the original manuscript (Gajer et al., 2012). Their cluster labeled as cluster IV-A disappears, being  
299 distributed among the other bigger clusters; approximately half of samples go to cluster I (our cluster  
300 no.4), some go to IV-B (our cluster no.3), and a few to cluster III (our cluster no.1). We note that, using  
301 our algorithm, the Prediction Strength decreases dramatically when passing from  $k=4$  to  $k=5$  clusters.  
302 Our cluster no.3 is that associated with bacterial vaginosis, and overlaps significantly with the disease  
303 cluster IV-B in Gajer et al. (2012)). The remaining clusters correspond to a (nominally) healthy vaginal  
304 microbiome.

### 305 Preterm infant gut microbiome sub-states

306 The dataset from La Rosa et al. (2014) has 922 samples and 29 OTUs at the class level. That collection  
307 includes data from 58 preterm babies, along different time points, for their first month and a half of life.  
308 Dataset details and availability are provided in the Data Citation section.

309 **Clustering assessment:** Without any previous attempt to distribute samples into groups for this  
310 dataset (La Rosa et al., 2014), our robust clustering methodology determined that there were optimally 4  
311 clusters that could be robustly partitioned (see Fig 1.4). The highest SI value (0.749) is achieved with  
312 PAM algorithm and Morisita-Horn metric for  $k=4$ , with all remaining metrics higher than the SI threshold.  
313 The robustness and stability of these 4 clusters are also verified by outperforming the Prediction Strength  
314 and Jaccard similarity limits ( $0.897 > 0.8$  and  $0.911 > 0.75$ , respectively).

315 **Cluster interpretation:** When we analyse the microbial composition of the 4 clusters shown in  
316 Fig 2.D, we found that cluster no.2 contains ~50% of the samples, cluster no.1 contains ~25%, cluster  
317 no.3 ~20% and cluster no.4 has <5% of the samples. Cluster no.3 appears to include the set of youngest  
318 babies (see the darkest squares in Fig 2.D); cluster no.1 the oldest babies (see the clearest circles); and  
319 cluster no.2 those being those of intermediate age. Analyzing the microbial composition of samples in  
320 each cluster, we found cluster no.1 and 3 are mainly enriched in Firmicutes, cluster 2 in Proteobacteria and  
321 cluster 4 in Bacteroidetes. This group distribution is in agreement with the La Rosa et al. (2014) results,  
322 where they suggest a beginning-of-life with primarily Bacilli (phylum: Firmicutes, as in our cluster no.3  
323 with the youngest babies); subsequently, there would have a Gammaproteobacteria prevalence (phylum:  
324 Proteobacteria, as in our cluster no.2); and finally, the infants would have Clostridia as the dominant  
325 species (phylum: Firmicutes, corresponding to our cluster no.1). We could not determine a biological  
326 association for the small cluster 4, based on the metadata captured by (La Rosa et al., 2014).

### 327 Taxa subset

328 In this section, we analyze what happens when we take distinct subsets of taxa and apply our approach to  
 329 find robust clusters in the different datasets. First, we select only the dominant taxa, that is a percentage  
 330 (exactly we took the 1%) of the most frequent taxa; and also the complementary subset with the non-  
 331 dominant taxa (number of taxa available in table 1). Second, we aggregate taxa at a higher resolution,  
 332 i.e. at genus taxonomic level, when possible. Then, we again build clusters with all, dominant and  
 333 non-dominant taxa at this genus level to compare with the previous results at species level, or the most  
 334 detailed available one (see table 2).

335 Table 1 shows a summary with the results comparing clustering with different taxa subsets. The first  
 336 row corresponds to the default results reported by our method (all taxa) and already explained in previous  
 337 sections. The other two rows in table 1 point out that the final number of sub-states trends towards only  
 338 plus/minus one variation when the clustering takes a subset of taxa. Mostly, clusters with dominant  
 339 taxa seems better according to clustering assessment measures. Moreover, it is relevant to note these  
 340 best evaluated clusters are found with a maximum of 13 taxa. Some studies have found that enterotypes  
 341 distinctions were primarily the result of different proportions of a small number of dominant species  
 342 (Gorvitovskaia et al., 2016), probably similar to our results with dominant taxa. Sometimes, the additional  
 343 appeared clusters could be outliers more than a new sub-state. For example, in Ballou et al. (2016) with  
 344 dominant taxa, in the third new cluster only there are 6 samples, from unrelated young chicks. Clusters  
 345 without those dominant taxa are clearly worse in assessment measures; even not finding robust clusters in  
 346 one case (Gajer et al. (2012)). However, some studies have reported relevant interactions for microbiome  
 347 dynamics among rare taxa (Claussen et al., 2017). So, these clusters could be useful in some particular  
 348 cases.

**Table 1. Robust clustering results with all, dominant and non-dominant taxa.** Clustering quality scores (SI>0.25 and (PS>0.8 or Jaccard>0.75)). Not clusters found in Gajer2012 with non-dominant taxa, due to not 2 distance measures with SI>threshold.

no.clusters SI\PS\Jaccard no.taxa	David2014	Ballou2016	Gajer2012	LaRosa201
<b>All</b>	3 0.60/0.95/0.99 4746	2 0.43/0.94/0.96 1583	4 0.73/0.93/0.99 298	4 0.75/0.90/0.91 29
<b>Dominant</b>	2 0.70/0.99/0.99 13	3 0.83/0.71/0.81 6	5 0.79/0.48/0.88 13	3 0.91/0.98/0.99 3
<b>Non-dominant</b>	3 0.60/0.97/0.99 4733	6 0.33/0.33/0.76 1577	- - 285	4 0.87/0.64/0.82 26

349 Table 2 summarizes the clustering results after aggregating taxa at genus level. Our procedure only  
 350 found clusters in two datasets, because of Gajer et al. (2012) dataset was not provided with taxonomic  
 351 information in the original publication, and La Rosa et al. (2014) dataset does not allow the taxa  
 352 simplification at genus level because the samples have taxonomy associated at a higher level (i.e. class  
 353 level). SI values are lower than before aggregation at genus level reporting weaker clusters, while PS and  
 354 Jaccard scores are preserved at high values, meaning high robustness in the new found sub-states. In many  
 355 studies, the OTU tables are aggregated at genus level, therefore this alternative way to find sub-states  
 356 could be useful in some specific scenarios.

357 Figure 3 shows the distribution of samples in clusters with the six considered alternative subsets of  
 358 taxa in the gut microbiome dataset (see supplementary figure S2 for corresponding results in the chick  
 359 gut dataset). In the bottom row (genus aggregation), in the first and second columns (all and dominant  
 360 taxa) the clusters are difficult to distinguish. The differences in the general shape of the scatterplots  
 361 among different cases is also due to the distance measure, being JSD in all the cases where there are  
 362 3 clusters. Apparently, it is difficult to say whether one of these three clustering configurations in 3  
 363 sub-states is clearly better than others. Hence, more knowledge or meta-data about the specific domain

**Table 2. Robust clustering results after genus aggregation with all, dominant and non-dominant taxa.** Clustering quality scores (SI>0.25 and (PS>0.8 or Jaccard>0.75))

no.clusters SI\PS\Jaccard no.taxa	David2014	Ballou2016
<b>All</b>	2 0.58/0.93/0.96 386	2 0.63/0.93/0.98 180
<b>Dominant</b>	2 0.58/0.85/0.96 10	2 0.67/0.96/0.99 9
<b>Non-dominant</b>	3 0.62/0.89/0.99 376	4 0.44/0.56/0.81 171

364 where sub-states would be applied might be necessary to conclude which clustering configuration is more  
365 suitable than others.

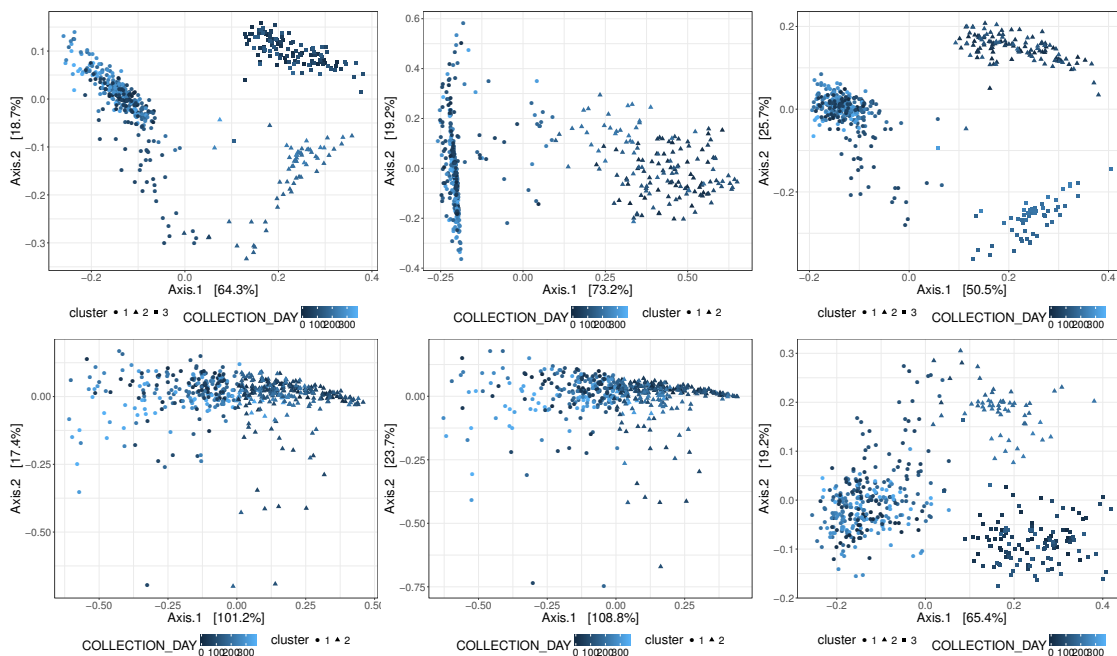


**Figure 3. Clusters in Human Gut with different number of taxa, represented as Principal Coordinates graphs.** Top row: default taxonomic level (i.e. species), bottom row: genus aggregation. Columns from left to right: all, dominant and non-dominant.

## 366 DISCUSSION

367 Our analysis suggests that, in general, an agglomerative approach (such as PAM) is more suitable than a  
368 hierarchical partitioning (such as Hclust) in our microbiome clustering scenario, where we are trying to  
369 optimize the number of distinct sub-states to make more precise biological associations, for example, for  
370 the purpose of defining biomarkers. As such, we attempt to avoid singletons or very small clusters (with  
371 size < 5). In our analyses, Hclust tends to often generate just 2 clusters, according to the limit established  
372 by the robustness PS score (see central columns of supplementary figure S1), leading us to suggest that it

373 is not suitable for this task. The final bootstrapping step, measured in Jaccard similarity terms, determines  
374 that PAM partitions represent valid and stable clusters, with almost all  $k$  values. This contrasts with  
375 Hclust, where many  $k$  values with different distance measures do not reach the minimum of 0.75 of mean  
376 Jaccard similarity. Additionally, PS seems to be the most restrictive score we can apply to discriminate  
377 between a viable partition of microbiome samples, and other non-robust possibilities where the scores fall  
378 below its threshold of 0.8 (see central columns of Figure 1). Regarding beta diversity measures, JSD and  
379 Morisita-Horn are the metrics that usually resulted in the highest SI values, in whatever number of taxa.

380 We want to contribute to standardization in microbiome, promoted by the International Human  
381 Microbiome Standards (IHMS) (Morton et al., 2017) and the Microbiome Quality Control Project  
382 (MBQC) (Costea et al., 2017) with a reproducible pipeline to find sub-states in longitudinal microbiome,  
383 and ensure comparability. We do not combine data from different studies, to avoid mix different ways of  
384 extracting DNA and pre-processing it, but we does combine samples from different subjects, increasing  
385 the diversity of the subjects and, consequently, their wider applicability.

386 Within the four datasets used in this manuscript, our novel method found varying numbers of  
387 microbiome sub-states depending on the particular dataset composition: one with 2 clusters (chick gut);  
388 another with 3 clusters (human gut); and two datasets with 4 clusters (vaginal microbiome and preterm  
389 infant gut). These results provide evidence that our algorithm is applicable to domains with a wide range  
390 of diversity and heterogeneity. There are many papers talking about stability and dynamics in microbiome,  
391 and many of them are focused in human gut microbiome, while our approach is wider, applicable to  
392 whatever microbiome. There is not an objective way to check the correctness of our cluster definition, due  
393 to a lack of gold standard datasets with groups definition. However, we find biologically-relevant clusters  
394 although our datasets were not designed to be analysed in this way, and are perhaps too small for this kind  
395 of analysis.

396 There are multiple choices when clustering metagenomics data, and someones do not consider them  
397 statistically significant enough grouped. However, the same weak statistics arised when clustering different  
398 bodysites, and the difference in microbiomes of distinct body sites is scientifically widely accepted (Costea  
399 et al., 2018). Moreover, even though the longitudinal microbiome data would evolve more continuously  
400 than in a discrete way, a discretization approach could be plausible as a simplification to make viable  
401 computational modeling analysis about the influence of external perturbations on microbiome dynamics.  
402 In fact, many real processes (including many biological ones) are not discrete in time, although they are  
403 simplified as discrete to allow their modeling to be studied with computational and mathematical models  
404 (Faust and Raes, 2012; Faust et al., 2015), as we are claiming in our proposal of clustering longitudinal  
405 microbiome data in sub-states.

406 In the result section, we compare the clustering decisions with different sets of taxa applied to real  
407 longitudinal metagenomics data. Focusing on less abundant taxa to characterize microbiome clusters  
408 is not a common practice, even though some studies highlight interesting events about that: Claussen  
409 et al. (2017) found there are interactions between low abundances (i.e. rare) taxa, and Martí et al. (2017)  
410 concludes that the most abundant taxa are less volatile than the less abundant ones. Thus, it could imply  
411 that giving importance to not-dominant species when sub-states definition, as our approach allows, could  
412 evince shifts in microbiome not visible using only-dominant-based sub-states. The default decision in  
413 our pipeline is with all the available taxa in the data, although different sets of taxa can be considered  
414 ( $\{\text{dominant, without dominant taxa}\} \times \{\text{genus or species level}\}$ ), allowing the users to select the clusters  
415 at the level most suitable to their goal.

416 The concept of a "microbiome biomarker" (Gorvitovskaia et al., 2016) aligns well which our observa-  
417 tions of microbiome sub-states being dependent on perturbations. In fact, our clustering pipeline is likely  
418 best-suited to identifying sub-states of dysbiosis or otherwise "perturbed" situations, and less suitable for  
419 studying non-perturbed steady-state microbiomes expressing more continuous dynamic changes (Gibbons  
420 et al., 2017) versus the discrete state-changes resulting from disease, dysbiosis or other perturbations.

## 421 CONCLUSIONS

422 This manuscript describes an automatic algorithm that determines a set of distinct microbiome sub-states  
423 in longitudinal data, given an available set of a particular cavity microbiome time series. Our novel  
424 methodology is characterized by a robust, objective, transparent and reproducible assessment of the  
425 quality of the identified sub-states. The algorithm is flexible with regards to the data source and taxa, and  
426 may be applied to a wide range of investigations over diverse species and intervention scenarios.

427 In summary, there is not an standard method to define clusters or sub-states in microbiome, even less in  
428 longitudinal microbiome datasets. After reviewing and analyzing many studies, with different procedures  
429 and distinct results about clustering gut microbiome datasets, Costea et al. (2018) concludes any procedure  
430 is not preferred versus others, but it depends on the conditions in each particular case, however all of them  
431 have allowed to carry out a particular microbiome analysis. Likely, the best procedure will depend on the  
432 posterior application of those clusters. Therefore, given there is not a universal standard, in our defined  
433 scenario about clustering longitudinal microbiome datasets of several subjects together, we decided to run  
434 a wide variety of those clustering procedures and to select the best one in each case, based on clustering  
435 assessment measures, to help users to take the decision, facilitating the use of the resulting sub-states.

436 As an additional outcome from our analyses, we make available the data files containing the sub-states  
437 we defined, to enhance the data provided by the datasets authors, and allow additional posterior analyses,  
438 for example, to elucidate the causes of transitions between different microbiome sub-states.

439 Natural variations and stress factors modify microbiota composition (Weiss and Hennet, 2017),  
440 however it is an open problem to discover which element(s) lead a specific shift and how and why that  
441 transitions happen. Thus, our new pipeline could help to develop novel methods to predict how to move  
442 from one to another of these microbiome sub-states depending on external perturbations.

#### 443 **Code and data availability**

444 Our algorithm, implemented in R, is freely available at GitHub: <https://github.com/wilkinsonlab/robust-clustering-metagenomics>. Our output data files are available at Zenodo: <http://doi.org/10.5281/zenodo.167376>

#### 446 **Data Citation**

447 This section describes the sources of the different input datasets.

##### 448 ***Human gut microbiome (David et al., 2014):***

449 • Metadata: David, L. et al. *Genome Biology*. Additional file 18: [https://static-content.springer.com/esm/art:10.1186/13059-016-0988-y/MediaObjects/13059\\_2016\\_988\\_MOESM18\\_ESM.csv](https://static-content.springer.com/esm/art:10.1186/13059-016-0988-y/MediaObjects/13059_2016_988_MOESM18_ESM.csv) or [http://web.mit.edu/ldavid/www/MF\\_David\\_FWD\\_LAD\\_2014\\_06\\_10.xlsx](http://web.mit.edu/ldavid/www/MF_David_FWD_LAD_2014_06_10.xlsx) (2014)

453 • OTU table: it was kindly shared by the authors in a personal communication

454 • Raw data: *EBI/ENA* ERP006059 (2014)

##### 455 ***Chick gut microbiome (Ballou et al., 2016):***

456 *Qiita* 10291 (2016)

##### 457 ***Vaginal microbiome (Gajer et al., 2012):***

458 • OTU table and metadata: Gajer P. et al. *Science* Supplementary table S2 (2012)

459 • Raw data: *SRA* SRA026073 (2012).

##### 460 ***Preterm infant gut microbiome (La Rosa et al., 2014):***

461 OTU table and metadata: La Rosa, P.S. et al. *PNAS* Supporting Information, Dataset\_S01: <http://www.pnas.org/lookup/suppl/doi:10.1073/pnas.1409497111/-/DCSupplemental/pnas.1409497111.sd01.xlsx>

#### 464 **ACKNOWLEDGEMENTS**

465 Thanks to the authors of David et al. (2014) for kindly providing the OTU table privately and to the  
466 authors of Ballou et al. (2016) for pleasantly answering our questions about their datasets and metadata.  
467 All authors had full access to all the data in the study and take responsibility for the integrity of the data  
468 and the accuracy of the data analysis.

## 469 REFERENCES

- 470 Arumugam, M., Raes, J., and al., E. (2011a). Enterotyping tutorial. <http://enterotype.embl.de>.
- 471 Arumugam, M., Raes, J., Pelletier, E., et al. (2011b). Enterotypes of the human gut microbiome. *Nature*,  
472 473(7346):174–80.
- 473 Ballou, A. L., Ali, R. A., Mendoza, M. A., Ellis, J. C., Hassan, H. M., Croom, W. J., and Koci, M. D.  
474 (2016). Development of the chick microbiome: How early exposure influences future microbial  
475 diversity. *Frontiers in Veterinary Science*, 3(2).
- 476 Barwell, L. J., Isaac, N. J. B., and Kunin, W. E. (2015). Measuring  $\beta$ -diversity with species abundance  
477 data. *Journal of Animal Ecology*, 84(4):1112–1122.
- 478 Bashan, A., Gibson, T. E., Friedman, J., Carey, V. J., Weiss, S. T., Hohmann, E. L., and Liu, Y.-Y. (2016).  
479 Universality of human microbial dynamics. *Nature*, 534(7606):259–262.
- 480 Bradley, P. H. and Pollard, K. S. (2017). Proteobacteria explain significant functional variability in the  
481 human gut microbiome. *Microbiome*, 5(1):36.
- 482 Chan, S. H. J., Simons, M. N., and Maranas, C. D. (2017). SteadyCom: Predicting microbial abundances  
483 while ensuring community stability. *PLOS Computational Biology*, 13(5):e1005539.
- 484 Claussen, J. C., Skiecevičienė, J., Wang, J., Rausch, P., Karlsen, T. H., Lieb, W., Baines, J. F., Franke,  
485 A., and Hütt, M.-T. (2017). Boolean analysis reveals systematic interactions among low-abundance  
486 species in the human gut microbiome. *PLOS Computational Biology*, 13(6):e1005361.
- 487 Costea, P. I., Hildebrand, F., Arumugam, M., Bäckhed, F., Blaser, M. J., Bushman, F. D., de Vos, W. M.,  
488 Ehrlich, S., Fraser, C. M., Hattori, M., Huttenhower, C., Jeffery, I. B., Knights, D., Lewis, J. D., Ley,  
489 R. E., Ochman, H., O'Toole, P. W., Quince, C., Relman, D. A., Shanahan, F., Sunagawa, S., Wang, J.,  
490 Weinstock, G. M., Wu, G. D., Zeller, G., Zhao, L., Raes, J., Knight, R., and Bork, P. (2018). Enterotypes  
491 in the landscape of gut microbial community composition. *Nature Microbiology*, 3(1):8–16.
- 492 Costea, P. I., Zeller, G., Sunagawa, S., Pelletier, E., Alberti, A., Levenez, F., Tramontano, M., Driessen,  
493 M., Hercog, R., Jung, F.-E., Kultima, J. R., Hayward, M. R., Coelho, L. P., Allen-Vercoe, E., Bertrand,  
494 L., Blaut, M., Brown, J. R. M., Carton, T., Cools-Portier, S., Daigneault, M., Derrien, M., Druesne,  
495 A., de Vos, W. M., Finlay, B. B., Flint, H. J., Guarner, F., Hattori, M., Heilig, H., Luna, R. A., van  
496 Hylckama Vlieg, J., Junick, J., Klymiuk, I., Langella, P., Le Chatelier, E., Mai, V., Manichanh, C.,  
497 Martin, J. C., Mery, C., Morita, H., O'Toole, P. W., Orvain, C., Patil, K. R., Penders, J., Persson, S.,  
498 Pons, N., Popova, M., Salonen, A., Saulnier, D., Scott, K. P., Singh, B., Slezak, K., Veiga, P., Versalovic,  
499 J., Zhao, L., Zoetendal, E. G., Ehrlich, S. D., Dore, J., and Bork, P. (2017). Towards standards for  
500 human fecal sample processing in metagenomic studies. *Nature Biotechnology*, 35(11):1069–1076.
- 501 David, L. A., Materna, A. C., Friedman, J., Campos-Baptista, M. I., Blackburn, M. C., Perrotta, A.,  
502 Erdman, S. E., and Alm, E. J. (2014). Host lifestyle affects human microbiota on daily timescales.  
503 *Genome biology*, 15(7):R89.
- 504 Ding, T. and Schloss, P. D. (2014). Dynamics and associations of microbial community types across the  
505 human body. *Nature*, 509(7500):357–60.
- 506 Faith, D. P., Minchin, P. R., and Belbin, L. (1987). Compositional dissimilarity as a robust measure of  
507 ecological distance. *Vegetatio*, 69(1-3):57–68.
- 508 Faust, K., Lahti, L., Gonze, D., de Vos, W. M., and Raes, J. (2015). Metagenomics meets time series  
509 analysis: unraveling microbial community dynamics. *Current Opinion in Microbiology*, 25:56–66.
- 510 Faust, K. and Raes, J. (2012). Microbial interactions: from networks to models. *Nature Reviews*  
511 *Microbiology*, 10(8):538–550.
- 512 Gajer, P., Brotman, R. M., Bai, G., Sakamoto, J., Schütte, U. M. E., Zhong, X., Koenig, S. S. K., Fu, L.,  
513 Ma, Z. S., Zhou, X., Abdo, Z., Forney, L. J., and Ravel, J. (2012). Temporal dynamics of the human  
514 vaginal microbiota. *Science translational medicine*, 4(132):132ra52.
- 515 Gibbons, S. M., Kearney, S. M., Smillie, C. S., and Alm, E. J. (2017). Two dynamic regimes in the human  
516 gut microbiome. *PLOS Computational Biology*, 13(2):e1005364.
- 517 Gilbert, J. A., Quinn, R. A., Debelius, J., Xu, Z. Z., Morton, J., Garg, N., Jansson, J. K., Dorrestein,  
518 P. C., and Knight, R. (2016). Microbiome-wide association studies link dynamic microbial consortia to  
519 disease. *Nature*, 535(7610):94–103.
- 520 Gorvitovskaia, A., Holmes, S. P., and Huse, S. M. (2016). Interpreting Prevotella and Bacteroides as  
521 biomarkers of diet and lifestyle. *Microbiome*, 4:15.
- 522 Hennig, C. (2007). Cluster-wise assessment of cluster stability. *Computational Statistics & Data Analysis*,  
523 52(1):258–271.

- 524 Hennig, C. (2008). Dissolution point and isolation robustness: Robustness criteria for general cluster  
525 analysis methods. *Journal of Multivariate Analysis*, 99(6):1154–1176.
- 526 Kaufman, L. and Rousseeuw, P. (1987). Clustering by means of medoids. In *Statistical Data Analysis*  
527 *Based on the L1 Norm and Related Methods*, pages 405–416.
- 528 Kaufman, L. and Rousseeuw, P. (1990). *Finding Groups in Data: An Introduction to Cluster Analysis*.  
529 Wiley-Interscience.
- 530 Koleff, P., Gaston, K. J., and Lennon, J. J. (2003). Measuring beta diversity for presence-absence data.  
531 *Journal of Animal Ecology*, 72(3):367–382.
- 532 Koren, O., Knights, D., Gonzalez, A., Waldron, L., Segata, N., Knight, R., Huttenhower, C., Ley, R. E.,  
533 Qin, J., Li, R., Raes, J., Arumugam, M., Burgdorf, K., Arumugam, M., Raes, J., Pelletier, E., Paslier,  
534 D. L., Yamada, T., Caporaso, J., Kuczynski, J., Stombaugh, J., Bittinger, K., Bushman, F., Filippo,  
535 C. D., Cavalieri, D., Paola, M. D., Ramazzotti, M., Poullet, J., Dethlefsen, L., Relman, D., McDonald,  
536 D., Price, M., Goodrich, J., Nawrocki, E., Desantis, T., Lozupone, C., Knight, R., Segata, N., Waldron,  
537 L., Ballarini, A., Narasimhan, V., Jousson, O., Tibshirani, R., Walther, G., Rousseeuw, P., Wu, G., Chen,  
538 J., Hoffmann, C., Bittinger, K., Chen, Y., Costello, E., Lauber, C., Hamady, M., Fierer, N., Gordon,  
539 J., Dominguez-Bello, M., Costello, E., Contreras, M., Magris, M., Hidalgo, G., Koenig, J., Spor, A.,  
540 Scalfone, N., Fricker, A., Stombaugh, J., Milligan, G., Cooper, M., Claesson, M., Jeffery, I., Conde,  
541 S., Power, S., O'Connor, E., Ravel, J., Gajer, P., Abdo, Z., Schneider, G., Koenig, S., Kuczynski, J.,  
542 Lauber, C., Walters, W., Parfrey, L., Clemente, J., Kumar, P., Brooker, M., Dowd, S., Camerlengo, T.,  
543 Caporaso, J., Lauber, C., Costello, E., Berg-Lyons, D., Gonzalez, A., Ley, R., Turnbaugh, P., Klein,  
544 S., Gordon, J., Turnbaugh, P., Hamady, M., Yatsunencko, T., Cantarel, B., Duncan, A., Costello, E.,  
545 Gordon, J., Secor, S., Knight, R., Crawford, P., Crowley, J., Sambandam, N., Muegge, B., Costello, E.,  
546 Jumpertz, R., Le, D., Turnbaugh, P., Trinidad, C., and Bogardus, C. (2013). A Guide to Enterotypes  
547 across the Human Body: Meta-Analysis of Microbial Community Structures in Human Microbiome  
548 Datasets. *PLOS Comput Biol*, 9(1):59–65.
- 549 La Rosa, P. S., Warner, B. B., Zhou, Y., Weinstock, G. M., Sodergren, E., Hall-Moore, C. M., Stevens,  
550 H. J., Bennett, W. E., Shaikh, N., Linneman, L. A., Hoffmann, J. A., Hamvas, A., Deych, E., Shands,  
551 B. A., Shannon, W. D., and Tarr, P. I. (2014). Patterned progression of bacterial populations in the  
552 premature infant gut. *Proceedings of the National Academy of Sciences*, 111(34):12522–12527.
- 553 MacDonald, N. J., Parks, D. H., and Beiko, R. G. (2012). Rapid identification of high-confidence  
554 taxonomic assignments for metagenomic data. *Nucleic Acids Research*, 40(14):e111–e111.
- 555 Martí, J. M., Martínez-Martínez, D., Rubio, T., Gracia, C., Peña, M., Latorre, A., Moya, A., and P. Garay,  
556 C. (2017). Health and Disease Imprinted in the Time Variability of the Human Microbiome. *mSystems*,  
557 2(2):e00144–16.
- 558 McDonald, D., Clemente, J. C., Kuczynski, J., Rideout, J. R., Stombaugh, J., Wendel, D., Wilke, A., Huse,  
559 S., Hufnagle, J., Meyer, F., Knight, R., and Caporaso, J. G. (2012). The Biological Observation Matrix  
560 (BIOM) format or: how I learned to stop worrying and love the ome-ome. *GigaScience*, 1(1):7.
- 561 McMurdie, P. J. and Holmes, S. (2013). phyloseq: An R package for reproducible interactive analysis and  
562 graphics of microbiome census data. *PLoS ONE*, 8(4):e61217.
- 563 Morton, J. T., Toran, L., Edlund, A., Metcalf, J. L., Lauber, C., and Knight, R. (2017). Uncovering the  
564 Horseshoe Effect in Microbial Analyses. *mSystems*, 2(1):e00166–16.
- 565 Oksanen, J., Blanchet, F. G., Kindt, R., Legendre, P., Minchin, P. R., O'Hara, R. B., Simpson, G. L.,  
566 Solymos, P., Stevens, M. H. H., and Wagner, H. (2015). *vegan: Community Ecology Package*. R  
567 package version 2.3-1.
- 568 Reynolds, A. P., Richards, G., de la Iglesia, B., and Rayward-Smith, V. J. (2006). Clustering Rules:  
569 A Comparison of Partitioning and Hierarchical Clustering Algorithms. *Journal of Mathematical*  
570 *Modelling and Algorithms*, 5(4):475–504.
- 571 Rousseeuw, P. J. (1987). Silhouettes: A graphical aid to the interpretation and validation of cluster  
572 analysis. *Journal of Computational and Applied Mathematics*, 20:53–65.
- 573 Shankar, J. (2017). Insights into study design and statistical analyses in translational microbiome studies.  
574 *Annals of Translational Medicine*, 5(12):249–249.
- 575 Stein, R. R., Bucci, V., Toussaint, N. C., Buffie, C. G., Räscht, G., Pamer, E. G., Sander, C., and Xavier,  
576 J. B. (2013). Ecological Modeling from Time-Series Inference: Insight into Dynamics and Stability of  
577 Intestinal Microbiota. *PLoS Computational Biology*, 9(12):e1003388.
- 578 Tibshirani, R. and Walther, G. (2005). Cluster Validation by Prediction Strength. *Journal of Computational*



- 579 and Graphical Statistics, 14(3):511–528.
- 580 Turrone, S., Rampelli, S., Biagi, E., Consolandi, C., Severgnini, M., Peano, C., Quercia, S., Soverini,  
581 M., Carbonero, F. G., Bianconi, G., Rettberg, P., Canganella, F., Brigidi, P., and Candela, M. (2017).  
582 Temporal dynamics of the gut microbiota in people sharing a confined environment, a 520-day ground-  
583 based space simulation, MARS500. Microbiome, 5(1):39.
- 584 Valseth, K., Nesbø, C. L., Easterday, W. R., Turner, W. C., Olsen, J. S., Stenseth, N. C., and Haverkamp,  
585 T. H. A. (2017). Temporal dynamics in microbial soil communities at anthrax carcass sites. BMC  
586 Microbiology, 17(1):206.
- 587 Weiss, G. A. and Hennes, T. (2017). Mechanisms and consequences of intestinal dysbiosis. Cellular and  
588 Molecular Life Sciences, 74(16):2959–2977.
- 589 Wolda, H. (1981). Similarity indices, sample size and diversity. Oecologia, 50(3):296–302.
- 590 Zhou, Y., Mihindukulasuriya, K. A., Gao, H., La Rosa, P. S., Wylie, K. M., Martin, J. C., Kota, K.,  
591 Shannon, W. D., Mitreva, M., Sodergren, E., and Weinstock, G. M. (2014). Exploration of bacterial  
592 community classes in major human habitats. Genome Biology, 15(5):R66.